A Vascular Targeted Pan Phosphoinositide 3-Kinase Inhibitor Prodrug, SF1126, with Antitumor and Antiangiogenic Activity

Joseph R. Garlich,[3] Pradip De,[1] Nandini Dey,[1] Jing Dong Su,[3] Xiaodong Peng,[3] Antoinette Miller,[3] Ravoori Murali,[4] Yiling Lu,[4] Gordon B. Mills,[4] Vikas Kundra,[4] H-K. Shu,[2] Qiong Peng,[1] and Donald L. Durden[1]

[1]Section of Hematology/Oncology, Department of Pediatrics, Aflac Cancer Center and Blood Disorders Service, Children's Healthcare of Atlanta and [2]Department of Radiation Oncology, Emory University School of Medicine, Atlanta, Georgia; [3]Semafore Pharmaceuticals, Indianapolis, Indiana; and [4]Department of Experimental Therapeutics, M. D. Anderson Cancer Center, Houston, Texas

Abstract

PTEN and the pan phosphoinositide 3-kinase (PI3K) inhibitor 2-(4-morpholinyl)-8-phenyl-4H-1benzopyran-4-one (LY294002) exert significant control over tumor-induced angiogenesis and tumor growth *in vivo*. The LY294002 compound is not a viable drug candidate due to poor pharmacologic variables of insolubility and short half-life. Herein, we describe the development and antitumor activity of a novel RGDS-conjugated LY294002 prodrug, termed SF1126, which is designed to exhibit increased solubility and bind to specific integrins within the tumor compartment, resulting in enhanced delivery of the active compound to the tumor vasculature and tumor. SF1126 is water soluble, has favorable pharmacokinetics, and is well tolerated in murine systems. The capacity of SF1126 to inhibit U87MG and PC3 tumor growth was enhanced by the RGDS integrin ($\alpha v\beta 3/\alpha 5\beta 1$) binding component, exhibiting increased activity compared with a false RADS-targeted prodrug, SF1326. Antitumor activity of SF1126 was associated with the pharmacokinetic accumulation of SF1126 in tumor tissue and the pharmacodynamic knockdown of phosphorylated AKT *in vivo*. Furthermore, SF1126 seems to exhibit both antitumor and antiangiogenic activity. The results support SF1126 as a viable pan PI3K inhibitor for phase I clinical trials in cancer and provide support for a new paradigm, the application of pan PI3K inhibitory prodrugs for the treatment of cancer. [Cancer Res 2008;68(1):206–15]

Introduction

The PI3K pathway is a target of significant interest in human cancer due to the high frequency and broad spectrum of aberrations in the pathway observed in human tumors. Multiple efforts are under way in academia and industry to develop clinically relevant inhibitors of this signaling pathway. To inhibit all classes of PI3K is to potentially take a larger percentage of these elements of tumor survival, proliferation, and angiogenesis out. Hence, we sought to develop a clinically viable small molecule inhibitor against all isoforms of PI3K (pan PI3K inhibitor). This manipulation, if successful, would be tantamount to the inhibition of a larger number of cell surface receptors, which would exert a powerful control over proliferation, migration, metastasis, apoptosis, and angiogenesis. Such a pan PI3K inhibitor, 2-(4-morpholinyl)-8-phenyl-4H-1benzopyran-4-one (LY294002) was reported by Vlahos over 10 years ago (1) and shown to block all classes of PI3K with the following IC_{50} values: (*a*) p110α, 720 nmol/L; (*b*) p110β, 306 nmol/L; (*c*) p110γ, 1.6 μmol/L; and (*d*) p110δ, 1.33 μmol/L (2, 3). It also inhibits a number of other PI3Ks, such as mTOR and DNAPK at similar levels. Over 3,000 peer-reviewed publications have described a large number of physiologic effects of this inhibitor on numerous components of mammalian signaling. It has been shown in a number of *in vivo* models to possess antitumor activity but suffers from poor pharmacokinetics (4), poor water solubility, and undesirable toxicity. The systemic administration of the pan PI3K inhibitor LY294002 results in potent antitumor and antiangiogenic activity *in vivo* (5, 6). Considering the published literature using this compound and its desirable inhibition properties, we were motivated to explore targeted conjugates that would overcome the limitations and provide for a desirable inhibitory profile.

Herein, we report the development of a clinically viable pan PI3K inhibitor, SF1126 for therapeutic application in cancer. We describe chemical methods which result in the conversion of the research compound LY294002, termed SF1101, to a well-tolerated water-soluble antitumor agent *in vivo*. The chemical design combines a targeting group which is an RGDS peptide–linked integrin-targeted ($\alpha v\beta 3/\alpha 5\beta 1$ targeted) linked to a small molecule inhibitor which inhibits all members of the PI3K family (termed pan PI3K inhibitor). The preclinical development of a pan PI3K inhibitor compared with an isoform-specific inhibitor is supported by our desire to gain a greater therapeutic effect on a larger number of survival, proliferative, and/or angiogenic signaling pathways downstream of multiple redundant cell surface receptors (7). There are eight known mammalian PI3Ks divided into three classes based on structure, function, and substrate specificity (8). For a cancer treatment paradigm, we sought to target all members of the PI3K family, including class Ia and Ib isoforms. We describe the evaluation of pharmacokinetic, pharmacodynamic, antitumor, and antiangiogenic activity *in vivo* of SF1126 demonstrating marked improvement over the parental compound LY294002.

Materials and Methods

Synthesis of prodrugs: SF1126 and SF1326. The full synthesis and characterization of SF1126 and SF1326 will be described elsewhere.[5]

Prodrug cleavage and pharmacokinetic studies. Plasma samples were obtained by centrifuging individual blood samples, immediately upon

[5] Unpublished observation.

Note: Supplementary data for this article are available at Cancer Research Online (http://cancerres.aacrjournals.org/).

Requests for reprints: Donald L. Durden, Aflac Cancer Center and Blood Disorders Service, Emory University School of Medicine, Atlanta, GA. Phone: 404-778-5118; E-mail: dldurde@emory.edu.

doi:10.1158/0008-5472.CAN-07-0669

collection, for each of the various time points outlined in the protocol at 13,000 rpm for 5 min in a Micromax 100 Centrifuge. A 100 μL aliquot of plasma was transferred to an Eppendorf tube containing 100 μL of 50% methanol in water acidified with 2% glacial acetic acid and phosphoric acid. The samples were then snap frozen with liquid nitrogen and transferred to a −80°C storage for later analysis of drug concentration. Tumor samples were collected at specific time points and flash frozen for later analysis. The analysis was performed using liquid chromatography with single-ion mass spectrometric detection (Shimadzu 2010 LCMS) for the individual species at 308 and 427 with 10% to 60% acetonitrile water gradient and 100 μL injection volume.

Animals for *in vivo* studies. Athymic female mice (CD-1 *nu/nu*, 20–25 g) were used for all of the *in vivo* tumor growth inhibition studies. Mice were purchased from Harlan or obtained from the NIH National Cancer Institute repository and housed in on a 12-h light/dark cycle with food and water *ad libitum* under specific pathogen-free conditions, according to the guidelines of the Association for the Assessment and Accreditation for Laboratory Animal Care, International. All of the *in vivo* studies were carried out under approved institutional experimental animal care and use protocols.

Tumor implantation. U87MG, U251MG glioma, or PC3 prostate cancer cell lines were purchased from American Type Culture Collection. The U251MG and LN229 glioma cell lines, stably transduced with the vIII epidermal growth factor receptor (EGFR) mutant, were prepared as described (9). The LN229 glioma cell line and LN229 cells transduced with a reporter plasmid containing six copies of the vascular endothelial growth factor (VEGF) promoter [hypoxic response element (HRE)–linked to the firefly luciferase reporter; provided by Dr. Erwin Van Meir; ref. 10]. Cells were cultured in DMEM medium supplemented with 10% fetal bovine serum (FBS), penicillin, and streptomycin at 37°C in an incubator with 5% CO_2.

Treatment of mice with SF1126 and SF1326. Animals bearing tumors of ~100 mm^3 in size were randomized into three groups receiving either vehicle (acidified sterile water diluent for SF1126 or SF1326), SF1126, or SF1326 via s.c. administration on the left flank for 3 weeks at a dose of 50 mg/kg and a frequency of thrice weekly. No untoward effects were noted in mice treated with SF1126, SF1326, or vehicle. Measurement of tumor volumes was performed in three coordinates using calipers.

Biochemical analysis. Evaluation of effect of PI3K inhibitors on AKT and hypoxia-inducible factor-1α (HIF-1α) activity. U937 cells and baboon endothelial cells ($5–10 \times 10^6$) in 10% FBS-PBS were treated with 10 μmol/L of SF1101, SF1126 (with RGD targeting moiety), and SF1326 (RAD-targeted prodrug derivative) for 30 min with gentle shaking with or without prepulse of 50 μmol/L RGD peptide (Biomol Research Lab., Inc.) for 15 min as indicated in the individual experiments. At the end of treatment, cells were solubilized with lysis buffer [50 mmol/L Tris-HCL (pH 7.6), 150 mmol/L NaCl, 100 mmol/L NaF, 1 mmol/L EDTA, 1 mmol/L EGTA, 0.05% NP40, 1% aprotinin, 0.01 mg/mL leupeptin, and 0.08 mmol/L phenylmethylsulfonyl fluoride] for Western blots. AKT kinase assays were performed using the AKT1/protein kinase B (PKB), an immunoprecipitation kinase assay kit (Upstate Biotechnology) following the instructions of the manufacturer as described (11).

HIF-1α transcription activity. To determine the effects of SF1126 on HIF-1α function, we used the LN229 glioma cell line, which is stably transduced with four copies of the VEGF HRE promoter sequence upstream of the firefly luciferase gene (4 × HRE VEGF HRE; ref. 10). The HRE response element is induced under hypoxic conditions (1% O_2 for 4 h), resulting in a robust activation of HIF-1α transcription activity (6-fold induction). The LN229 glioma cells were treated with SF1126 at concentrations ranging from 10 to 20 μmol/L for 15 min before placing cells into hypoxic chamber (1% O_2) for 4 h at 37°C.

CD31 immunohistochemistry. At the end of the efficacy studies, tumors were harvested and placed in optimum cutting temperature blocks for frozen section analysis or fixed in 10% buffered formalin and/or processed into paraffin. Sections of tumor tissue at 4-μm thickness were stained with rat anti-mouse CD31 antibody for detection of the murine tumor microvasculature (12).

Statistical analysis. The Student's *t* test was used to evaluate differences observed between experimental groups and to compare tumor volume differences between SF1126-treated and SF1326-treated mice and vehicle-treated controls.

Results

The pan PI3K inhibitor LY294002 has potent antitumor and antiangiogenic activities *in vivo* (5, 6). A further analysis of the chemical, pharmacokinetic, and toxicologic properties of LY294002 suggested that it would not be a viable drug (4). Hence, we set out to develop a clinically viable tumor-targeted prodrug form of LY294002/SF1101 that would be water soluble (for facile clinical administration) and would have a more favorable pharmacokinetic and safety profile and hence have greater anticancer efficacy. The LY294002/SF1101 compound has very poor water solubility (200 μmol/L) with a cLogP value of +2.6 (1). The RGDS-conjugated and RADS-conjugated prodrugs, termed SF1126 and SF1326, respectively, were prepared using a solid phase synthesis approach (Fig. 1). A solid phase organic synthesis procedure was established, and a biophysical characterization of the SF1126 and SF1326 compounds was performed and yielded very similar profiles for (*a*) water solubility profile (45 wt.%), (*b*) cleavage to the active moiety (Fig. 2), and (*c*) cLogP (−4.6).[5] It should be noted that SF1126 has no detectable PI3K inhibitory activity until hydrolyzed to SF1101, which is in line with the known structure-activity relationship known to be very sensitive to substitutions of the morpholino group (1).

The SF1126 and SF1326 prodrug compounds were designed to remain stable at acidic pH (pH < 5) and to spontaneously hydrolyze at physiologic pH. The spontaneous cleavage of SF1126 (Fig. 2*A*) or SF1326 (Fig. 2*B*) was determined at pH 7.0 *in vitro*. Importantly, the cleavage rate and extent to which the SF1101 active compound was liberated *in vitro* from SF1126 versus SF1326 was almost identical between the two compounds (compare *A* to *B*). The pharmacokinetics of SF1126 given by three different routes (i.m., i.v., or s.c.) was then determined as shown in Fig. 2*C*. It should be noted that Fig. 2*C* depicts the plasma levels of active PI3K inhibitor SF1101/LY294002. The results show that the prodrug SF1126 provides for a significant increase in plasma half-life of SF1101/LY294002 after the *in vivo* administration of SF1126 by multiple routes, especially the s.c. administration route. The parental SF1101/LY294002 compound has a plasma half-life of <15 min (4) compared with the extended release of SF1101 from SF1126, which is observed with a half life of >1 h. In the same mice, we determined the effects of each mode of administration on plasma glucose levels (*D*) as the PI3K pathway mediates the effects of signaling through the insulin receptor and also modulates the GLUT1/4 transporter translocation to the cell membrane to enable glucose uptake. A transient pharmacodynamic effect of SF1126 was observed on plasma glucose, which lasts for ~2 h and spontaneously resolves by 3 to 4 h (Fig. 2*D*). These results provide evidence that our targeting strategy has improved the pharmacokinetic profile for the delivery of SF1101 and potentially suggest that the plasma glucose increase observed shortly after a therapeutic dose of SF1126 may serve as initial pharmacodynamic variable to follow in patients as we enter phase 1 clinical trials.

Because SF1126 has an RGDS-targeting moiety, the inhibitory effects of this drug in cell-based assays with limited exposure times should be at least partially blocked by the prepulsing with RGD peptide by virtue of occupying the RGDS-binding sites of the αvβ3/αvβ5 and α5β1. Hence, we have studied the effect of

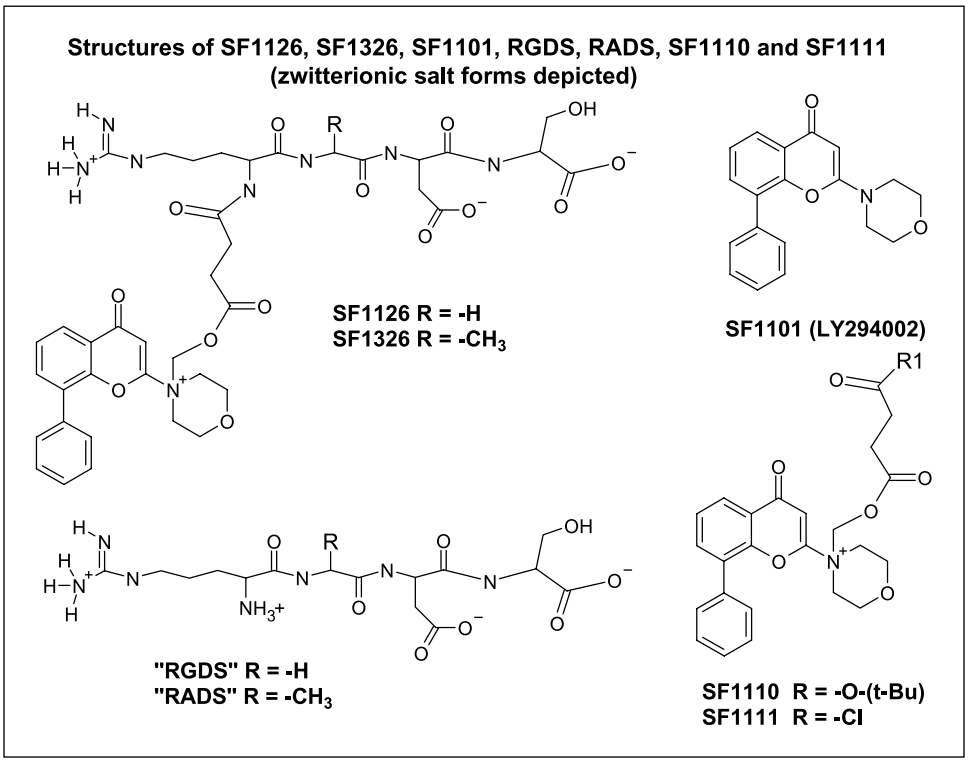

Figure 1. Structure of SF1126. The preparation of a vascular-targeted RGDS-conjugated prodrug SF1126 and RADS-conjugated SF1326 control. The SF1101, SF1110, SF1126, and SF1326 compounds were prepared as described in Materials and Methods. Upon cleavage at neutral pH, SF1126 or SF1326 spontaneously cleave to release the SF1101 active chemical moiety to inhibit PI3K activity.

prepulsing of RGDS peptide on the inhibition of phosphorylated AKT (p-AKT; levels of p-AKT and *in vitro* AKT kinase activity) after treatment with SF1101/LY294002, SF1126, and SF1326. We performed a prepulsing of cells with RGDS peptide for 15 min to occupy all available receptors, followed by brief washing, followed by a 20-min pulse with SF1101, SF1126, or SF1326, followed by washing, and then prepared lysates to examine pharmacodynamic effects. The data show that the inhibition of p-AKT after SF1126 treatment was blocked by the prepulse of 50 μmol/L of RGDS peptide for 15 min in both U937 cells and primate-derived endothelial cells (Fig. 3*A* and *B*). In contrast, a pulse of RGDS peptide before treatment with SF1101/LY294002 or SF1326 failed to block the inhibition of p-AKT. Interestingly, the RADS conjugate SF1326 is not affected by preincubation with RGDS however short pulses with SF1326 do result in significant inhibition of p-AKT, a result which suggests that the RADS conjugate may associate with cell surface receptors in an RGDS-independent manner. From these data, we conclude that SF1126 has a potent PI3K inhibitory effect (as observed by the inhibition of AKT phosphorylation) as it converts from SF1126 to SF1101/LY294002. The fact that this inhibitory action of SF1126 can be specifically blocked by a prepulse of RGDS peptide confirms that the activity of SF1126 under these conditions is at least partly dependent upon the RGDS peptide moiety binding to cells. To further confirm the importance of the RGDS targeting moiety on SF1126 on tumor cells, we used a more sensitive *in vitro* kinase assay for AKT kinase suppression. Unlike the p-AKT Western blot that shows only a dynamic range of 2-fold to 3-fold, the *in vitro* kinase assay shows a 10,000-fold difference in the presence of SF1126. The capacity of SF1126 to suppress the *in vitro* kinase activity of AKT in U937 cells is blocked 90% compared with a 5% inhibition in the presence of RGDS. Comparatively, the effect of RGDS on SF1101/LY294002 or SF1326 is minimal, if any. The effect of PI3K inhibition by SF1101, SF1126, and SF1326 was studied using levels of phosphorylated Ser^{473}-AKT and *in vitro* AKT kinase as readouts in both human myeloid cell lines and primate primary endothelial cells (Fig. 3). Figure 3*A* shows that a 10 μmol/L concentration of SF1126 or SF1101/LY294002 inhibited p-AKT (under standard serum conditions, 10% FBS) as determined by Western blot. The data show that AKT kinase activity was significantly blocked (>25-fold) after the treatment of 10 μmol/L of SF1101/LY294002, SF1126, or SF1326 (Fig. 3*C*). From these data, we conclude that the RGDS targeting module contributes to the pharmacodynamic activity of this prodrug.

The marked difference in the AKT inhibitory activity of SF1126 versus SF1326 under conditions where we pretreated with RGDS peptide *in vitro* led us to design a series of *in vivo* experiments comparing SF1126, at equivalent doses and timing, with the false targeted SF1326 compound in two different *in vivo* xenograft models for antitumor efficacy. We sought to determine if efficacy would correlate with tumor delivery of SF1101/LY294002 *in vivo*. The results show that SF1126 displays a greatly enhanced *in vivo* efficacy against a glioma subcutaneous xenograft model (U87MG cell line) versus SF1326, the "false-targeted" version of SF1126 (Fig. 4*A* and *D*). In other experiments, we show that treatment of tumor-bearing mice with an equimolar amount of RGDS moiety of SF1126, termed SF1174, has no significant antitumor activity *in vivo* (Supplementary Fig. S3). SF1126 displayed greater antitumor activity compared with SF1326 against the prostate cancer cell line (PC-3) in nude mice (Fig. 4*B*). The results show marked single agent antitumor efficacy of the SF1126 compared with SF1326. SF1126 reduced tumor growth by 76% versus 23% reduction noted with SF1326. Tumor growth remained depressed for substantial period after cessation of treatment regimen. We

have also shown that SF1126 has marked antitumor activity in other glioma models, LN229 and LN229vIII, and xenograft models, U251 and U251vIII (Fig. 6 and Supplementary Figs. S1*B, C* and S4).

We performed liquid chromatography–mass spectrometry analysis of plasma and tumor tissue to quantitate tissue levels of these inhibitors in an effort to correlate tumor response to enhanced tumor uptake. The results show that unlike the parental SF1101/LY294002 molecule (which has a half life of <10 min; not shown), the SF1126 prodrug has a plasma half-life of 1 to 2 h and releases the SF1101 active moiety into plasma and tumor compartment over a period of 2 to 4 h (Fig. 4*C*). By measuring the amount of SF1101 found in the tumor at 2-h postinjection, we show that the tumor uptake of SF1126 is increased by a factor of 6-fold or 4-fold in U87MG versus PC3 tumors, respectively, above serum levels 2 h after s.c. administration of the prodrug consistent with the capacity of SF1126 to target the tumor site preferentially over systemic levels for at least 2 h. It should be noted that tumor concentrations of SF1101 approximating 30 μmol/L are observed at 2 h postinjection of 50 mg/kg of SF1126. These concentrations are well above the enzymatic IC_{50} values for all PI3K isoforms. From these data, we concluded that SF1126 has a favorable pharmacokinetic and chemical profile for further testing *in vitro* and *in vivo* and that the SF1126 selectively accumulates within the tumor tissue. The amount of SF1101 found in the tumor is statistically more by a factor of 2 after administration of SF1126 when compared with the administration of SF1326 in tumor-bearing mice (Fig. 4*C*).

In both tumor models, the increased efficacy associated with SF1126 versus SF1326 was directly correlated with augmented levels of the SF1101/LY294002 observed within the tumor tissue, a result which provides *in vivo* evidence for the capacity of SF1126 to deliver more drug to the tumor site (2-fold increase; Fig. 4*C*). SF1126 showed significantly improved *in vivo* efficacy (inhibition of tumor growth) versus the false-targeted SF1326 ($P = 0.0025$) although both were effective relative to the control group ($P < 0.0001$ and $P = 0.005$, respectively). It should be noted that both SF1126 and SF1326 differ only in an alanine substitution for glycine in the tetrapeptide piece (Fig. 1) and convert at the same rate to release the same amount of the SF1101/LY294002 PI3K inhibitor (Fig. 2). This remarkable difference in one methyl group encodes the RGD recognition receptor-binding ability to αvβ3/α5β1 integrin of SF1126 *in vivo*. After the initiation of SF1126 therapy, PC3 prostate tumor tissue samples were obtained for reverse-phase protein array analysis as described (13) and processed to detect levels of p-AKT, S6 kinase, and phosphorylated

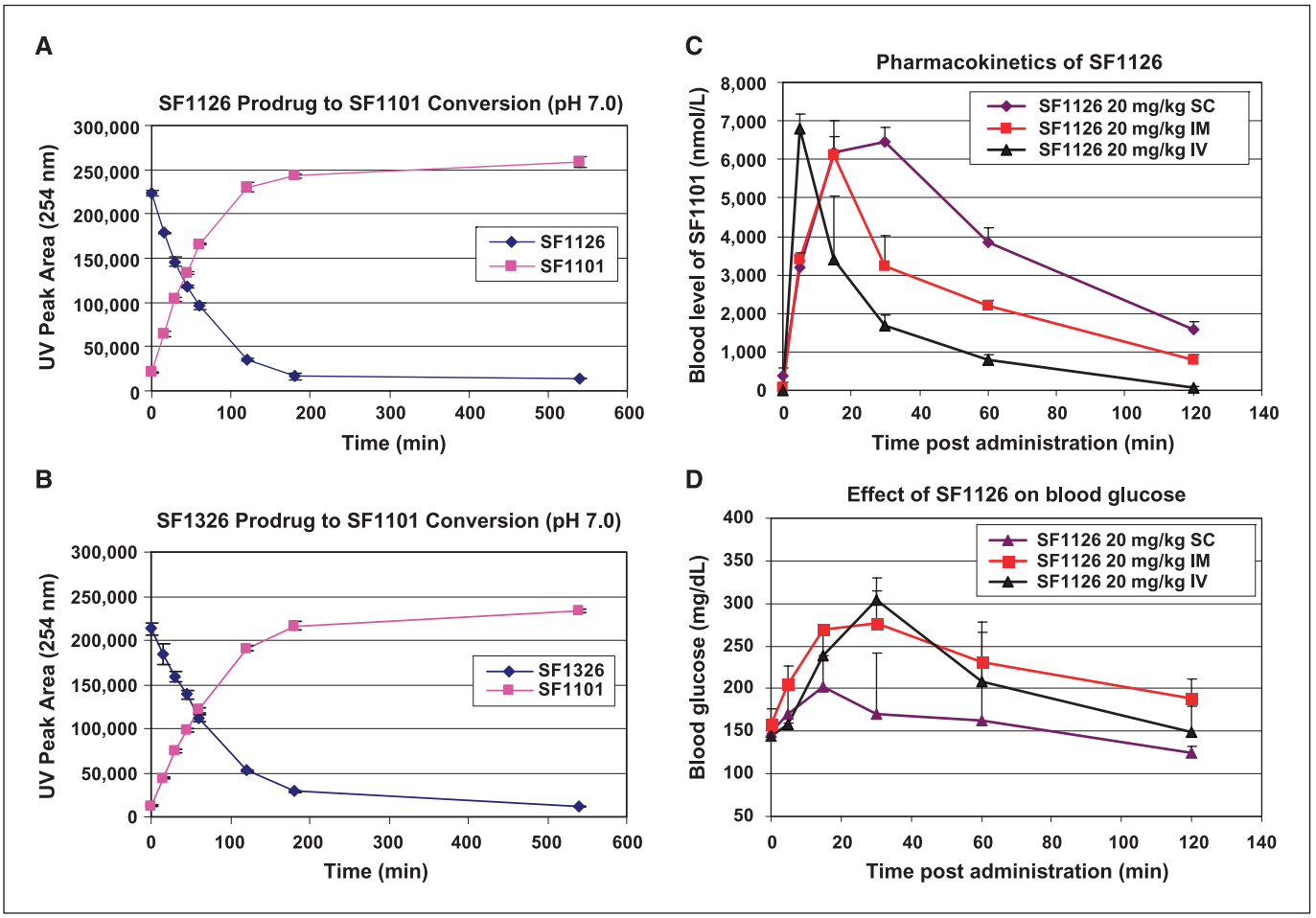

Figure 2. Cleavage of prodrugs SF1126 and SF1326 to SF1101. *In vitro* cleavage of SF1126 or SF1326 prodrugs. The spontaneous conversion of SF1126 (*A*) or SF1326 (*B*) to SF1101 was determined at neutral pH 7.0 using liquid chromatography–mass spectrometry analysis. The conversion rate for the two prodrug forms was similar. *C,* pharmacokinetics of SF1126 measuring SF1101. *D,* effect of SF1126 administration on plasma glucose concentrations after i.v., s.c., or i.m. administration.

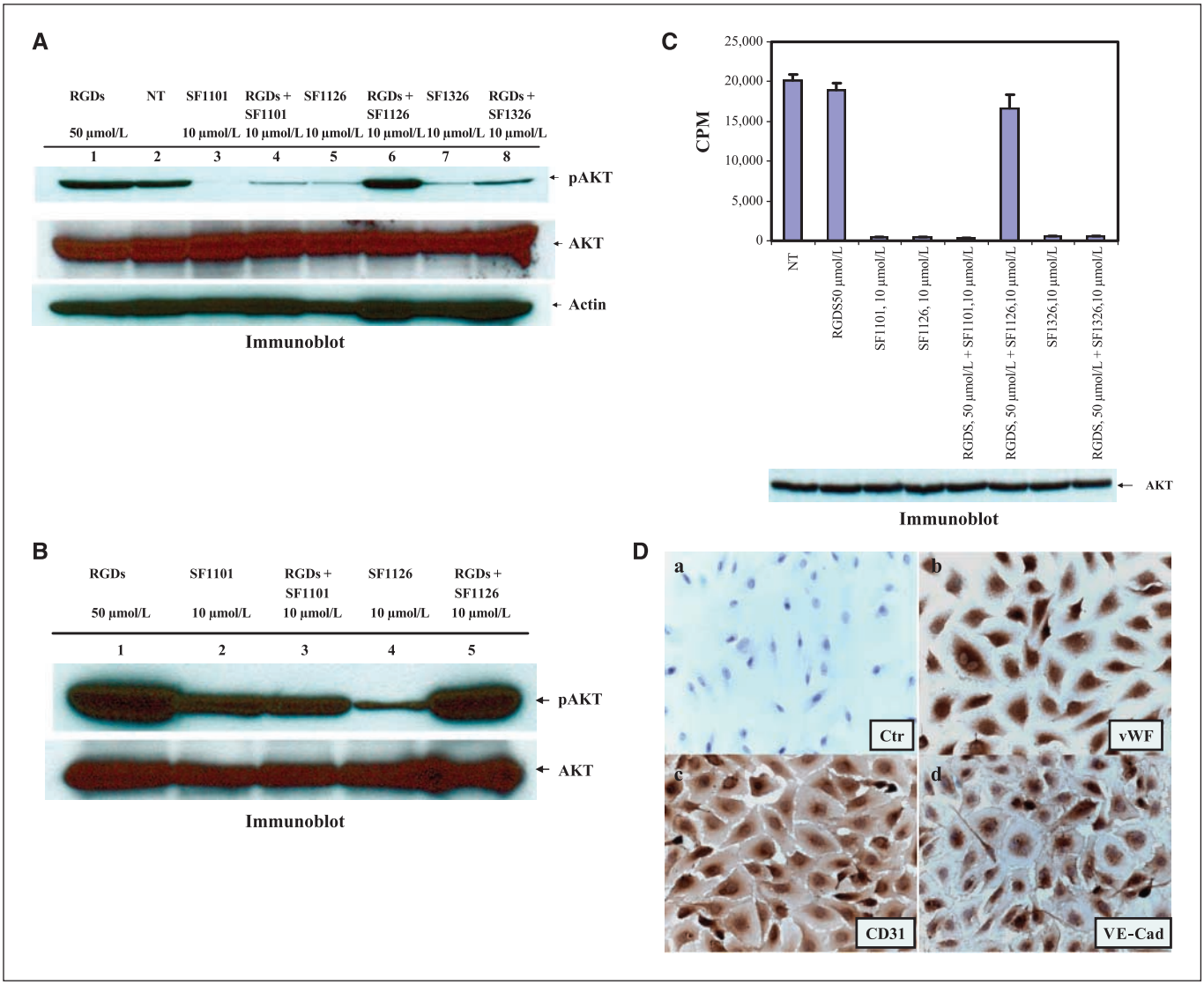

Figure 3. Evidence for *in vitro* pharmacodynamic RGDS-targeting capacity of SF1126 against AKT activation. *A,* Effect of prepulse of RGDS peptide on SF1101-treated, SF1126-treated, and SF1326-treated inhibition of p-AKT in a myeloid cell line (U937 cell). Cells were prepulsed with 50 μmol/L RGDS peptide for 15 min, washed in PBS, and treated with 10 μmol/L of SF1101, SF1126, and SF1326 for 30 min (in 10% FBS-PBS). Whole-cell lysates were probed with anti–phosphorylated Ser^{473}-AKT antibody (*top*). Probing with anti-AKT antibody served as loading control (*bottom*). Result shows that SF1126-mediated inhibition of p-AKT was blocked by the prepulse of RGDS peptide. *B,* effect of prepulse of RGDS peptide on SF1101-treated and SF1126-treated inhibition of p-AKT in primary circulating primate progenitor endothelial cells. Cells were treated with 10 μmol/L of SF1101 and SF1126 for 30 min in 10% FBS-PBS. RGDS peptide (50 μmol/L) was prepulsed for 15 min. Whole-cell lysates were probed with anti–phosphorylated Ser^{473} AKT antibody (*top*). Probing with anti-AKT antibody served as loading control (*bottom*). Result shows that SF1126-mediated inhibition of p-AKT was blocked by the prepulse of RGDS peptide. *C, in vitro* kinase assay of AKT immunoprecipitated from U937 cells. Effect of prepulse of RGDS peptide on SF1101-induced, SF1126-induced, and SF1326-induced inhibition of AKT kinase activity in U937 cells. Kinase activity of AKT was determined by *in vitro* assay using the AKT substrate peptide RPRAATF. Phosphotransferase activity of AKT from the treated cells was measured in immunocomplex formed between the AKT/PKBα PH domain antibody and active AKT/PKB as described in Materials and Methods. *Columns,* means of γ ^{32}P incorporation (in cpm) for three independent experiments; *bars,* SD (*top*). Western blots were carried out the same way, except immunoprecipitates were boiled in Laemmli buffer, run on a 10% SDS-PAGE gel, and probed with anti-AKT (*bottom*). Results show that the inhibition of p-AKT after the treatment of SF1126 was significantly protected by the prepulse of RGDS peptide. *D,* immunohistochemical characterization of primate endothelial cells was performed. *a,* isotype control antibody for *b* vWF; *b,* vWF specific antibody staining; *c,* VE cadherin-specific antibody staining; *d,* CD31 monoclonal antibody staining of endothelial cells.

$p27^{kip1}$ as a downstream readout of AKT inhibition at different time points after SF1126 administration (Supplementary Fig. S1*A*). The results from these experiments reveal prolonged pharmacodynamic knockdown of p-AKT and S6 kinase after SF1126 administration for up to 18 h after the administration of this compound. In contrast, the phosphorylated p27 (T157) was markedly reduced at the 4-h time point but rebounded above control levels at 18 h after administration of SF1126. In another glioma xenograft model, we used the U251MG or U251MG vIII glioma cell lines implanted into nude mice treated with SF1126 (Supplementary Fig. S1). Tumor cells transduced with EGFR vIII display augmented proliferation and induced activation of AKT in the absence of ligand (9). The vIII mutation of the EGFR involves a deletion of part of extracellular and cytoplasmic domains (deletion of exons 2–7), such that the receptor does not bind ligand and is constitutively active (14). We then correlated the response of tumor to SF1126 with a pharmacodynamic analysis of p-AKT levels and total AKT levels in tumor tissue (three controls and two SF1126-treated mice)

obtained 12 h after the last injection with SF1126 versus vehicle (Supplementary Fig. S1*D*). The results of these experiments show significant pharmacodynamic knockdown of p-AKT (2-fold to 3-fold reduction in p-AKT) in the SF1126-treated tumors.

To further evaluate the pharmacodynamic activity of SF1126 in another tumor model, we examined its activity in the MDA-MB-468 orthotopic mouse mammary tumor model (Fig. 5). MDA-MB-468 human breast carcinoma cells were injected into the mammary fat pad of nude mice. Mice were treated with 25 or 50 mg/kg/dose of SF1126 thrice weekly. Next, because the PI3K-AKT signaling axis is a known regulator of the GLUT1, GLUT3, and GLUT4, known glucose transporters in mammalian cells (15), we used ^{18}FDG–positron emission tomography (PET) imaging to evaluate the long-term effects of SF1126 on MDA-468 tumors. The MDA-MB-468 orthotopic mammary tumor model was used to determine if FDG-PET imaging could serve as a noninvasive surrogate marker for response to SF1126. Mice implanted with MDA-MB-468 tumors were treated for 3 weeks with SF1126 (25 or 50 mg/kg/dose MWF dosing; Fig. 5*A*). No increase in activity was noted at the higher dose, possibly indicating that the maximum biological effective dose is 25 mg/kg. At the end of treatment regimen, mice were given an injection of SF1126, and ^{18}FDG-PET imaging was performed 2 h later (Fig. 5*B*). The effects of SF1126 on tumor growth in this instance can be measured and quantitated by this imaging modality (Fig. 5*C*).

It has been suggested that tumors, which are transformed via the activation of the PI3K signaling axis, may be more sensitive to inhibitors of this pathway (16–18). This notion is supported by both laboratory and clinical observations, wherein tumors which have incurred mutations, for example, in EGFR or FLT3, are more sensitive to inhibitors of these receptor tyrosine kinases. To address this important question, we used isogenic tumor cell lines manipulated in different ways to display activation of PI3K-AKT to examine this important question, including (*a*) DOV13 ovarian carcinoma cell line transduced with activated p110α or myristoylated AKT and (*b*) LN229 glioma cells stably transduced with empty vector versus the mutated EGFR vIII (9). These different cell lines activated directly or indirectly for PI3K-AKT signaling were evaluated *in vitro* or *in vivo* for sensitivity to SF1126 (Fig. 6). DOV13 cells transduced with activated p110α p110CAAX were more sensitive to SF1126 than were the caAKT-transduced or parental p110α wild-type cell lines (Fig. 6*A*). Finally, the LN229 were compared *in vivo* to LN229 vIII cells for sensitivity to SF1126. The results show a 3-fold greater response of LN229 vIII tumors to SF1126 compared with the parental LN229 cell line (Fig. 6*C* versus *B*). The LN229 vIII displays a 4-fold increase in baseline p-AKT compared with LN229 cells (Fig. 6*D*; ref. 9). Interestingly, both p-AKT and phosphorylated extracellular signal-regulated kinase are suppressed by SF1101 and SF1126 in LN229 cells. A similar observation was

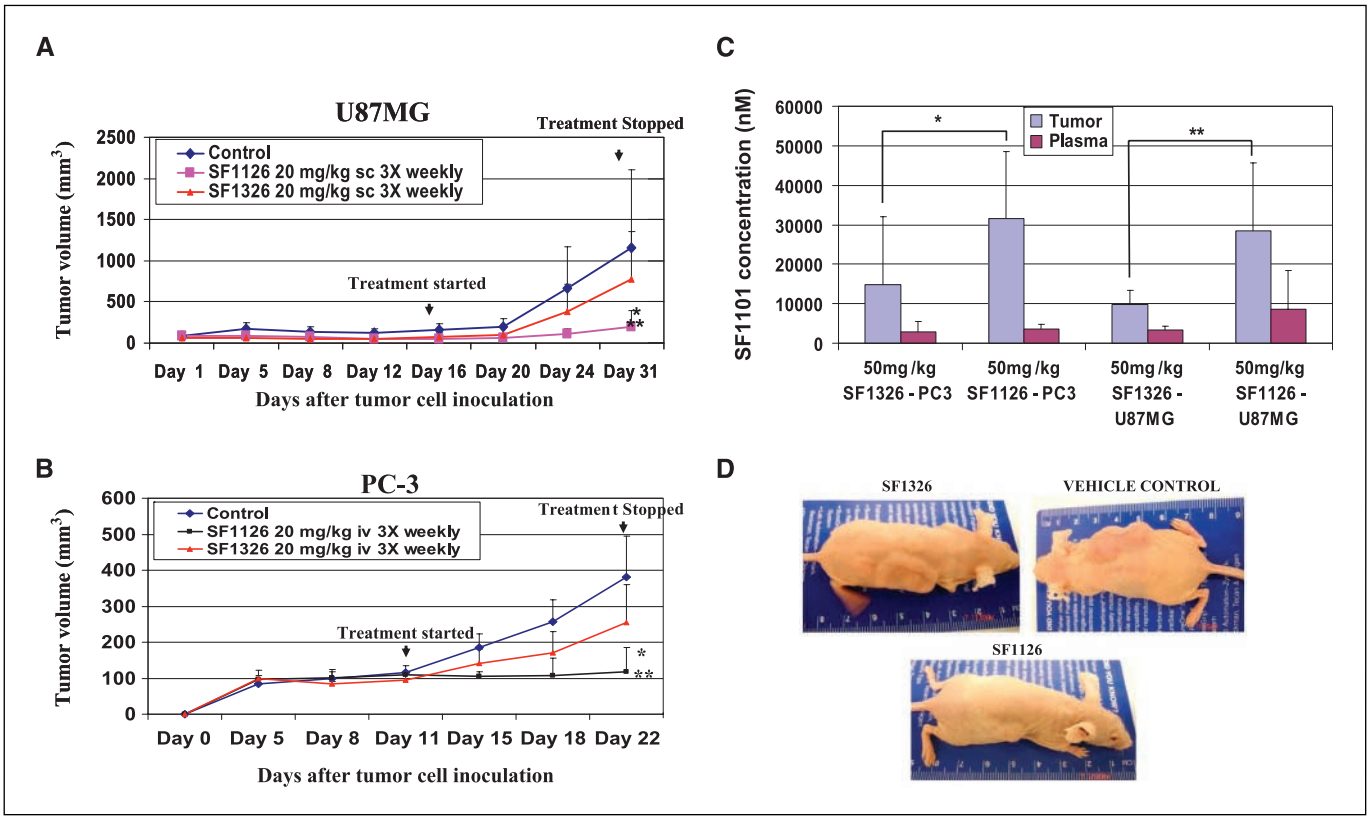

Figure 4. Correlation of antitumor activity of SF1126 versus SF1326 *in vivo* with augmented delivery of SF1101 to tumor tissue. *A*, comparison of SF1126 integrin targeted prodrug to the RADS-nontargeted inhibitor (SF1326) was performed. Briefly, these two compounds display similar cleavage rates to liberate the active compound LY294002 under physiologic conditions *in vitro* and *in vivo* (not shown). Nude mice implanted with U87MG or PC3 tumor cells s.c. were treated with equivalent doses of SF1126 versus SF1326 versus vehicle control. Tumor volumes were measured as shown. *A,* U87MG s.c. xenografts respond better to SF1126 compared with SF1326 as measured on day 31; $P < 0.001$. *B,* in the PC3 xenograft model, SF1126 has significantly greater antitumor activity compared with SF1326; $P < 0.008$, compare SF1126 to SF1326, day 22. *C,* nude mice bearing U87MG or PC3 tumors were injected at the left flank with 50 mg/kg/dose of either SF1126 or SF1326. After 2 h, mice were sacrificed and tumor excised, flash frozen for extraction of SF1101. Plasma samples were immediately obtained, acidified to stop conversion of SF1126 to SF1101, and were processed for high performance liquid chromatography–mass spectrometry analysis. *, $P < 0.05$; **, $P < 0.01$. *D,* photographs of U87MG tumors in mice treated with vehicle, SF1326, or SF1126.

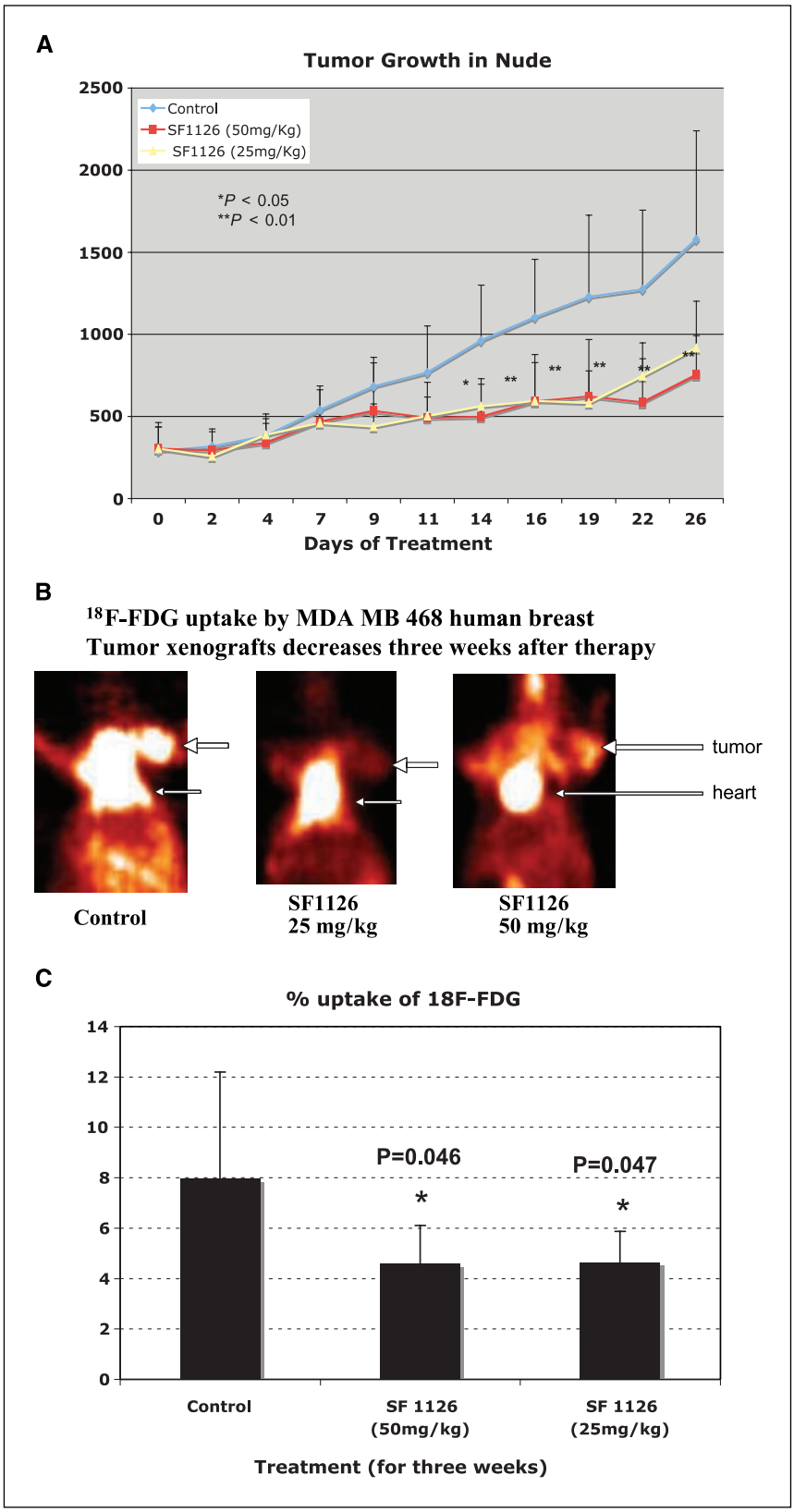

Figure 5. Pharmacodynamic monitoring of SF1126 activity using tumor tissue arrays and ^{18}FDG-PET in MDA-468 tumor model. *A,* SF1126 has antitumor activity in an orthotopic MDA-MB-468 mammary tumor model. *B,* ^{18}FDG-PET imaging of mice with MDA-468 tumors 2 h after the final dose of SF1126. SUV was determined for mammary fat pad tumor after injection of control diluent or SF1126 (25/mg/kg) s.c. after 2 h. *C,* quantitation of ^{18}FDG PET (SUV) signal of experiment in *C*.

made comparing the response of U251MG versus U251MG vIII cell line with SF1126 as shown in Supplementary Fig. S1*B* and *C*.

Several reports in the literature suggest that PTEN and PI3K inhibitors can block angiogenesis (6, 12). The mechanisms for antiangiogenic activity of pan PI3K inhibitors are not completely clear but seem to involve the coordinate regulation of proangiogenic and antiangiogenic effectors, such as thrombospondin-1, HIF-1α, VEGF, and others (12, 19). PTEN and PI3K have been

shown to regulate the transcription factor HIF-1α, a control point for the hypoxic induction of VEGF (19–21). As mentioned above, the SF1126 is RGD targeted to angiogenic integrins αvβ3, αvβ5, and α5β1; hence, it might be expected that this targeted prodrug will display antiangiogenic activity. To investigate the effects of the SF1126 on angiogenesis, we evaluated its effects on the hypoxic stabilization of HIF-1α and on HIF-1α transcription under hypoxic conditions in glioma cells. As shown in Supplementary Fig. S2, the results show that SF1126 blocks HIF-1α accumulation and profoundly inhibits HIF-1α transcription activity in LN229 glioma cells (90% suppression). Furthermore, we evaluated the effects of SF1126 on the capacity of LN229 vIII tumor cells to recruit a blood supply *in vivo* during thrice weekly of treatments with SF1126 at 50 mg/kg (Supplementary Fig. S2*C*). A quantitation of microvessel density in control versus SF1126-treated tumors showed a 72% decrease in MVD in SF1126*treated tumors, suggesting that this treatment has significant antiangiogenic properties *in vivo*. The antiangiogenic activity of SF1126 correlates with a block in the HIF-1α–VEGF signaling in the tumor cell. Moreover, an analysis of the effects of SF1126 in 6 of 11 xenograft models (data not shown) shows potent inhibition of tumor-induced angiogenesis *in vivo*.

Previous observations from our laboratory and other investigators suggest that pan PI3K inhibitors will sensitize tumor cells to chemotherapeutic agents and radiation (9, 22–28). To test this idea *in vivo*, we investigated the antitumor activity of combining pan PI3K inhibition with a cytotoxic agent targeting the tubulin/microtubule system taxotere (Supplementary Fig. S4). PC3 tumors treated with taxotere at 6 mg/kg/dose × 3 doses show reduced rate of growth compared with untreated control mice as do animals treated with SF1126 alone. PC3 tumors treated with a combination of taxotere followed by SF1126 show dramatic induction of tumor regression to an almost undetectable tumor volume by day 67.

Discussion

The class Ia and Ib PI3Ks are all involved in the regulation of a large number of important signaling events downstream of the PI3K-AKT kinase cascade including, but not restricted to, (*a*) mdm2-p53 axis (6), (*b*) IKKα–nuclear factor-κB pathway (29), (*c*) PAR-4

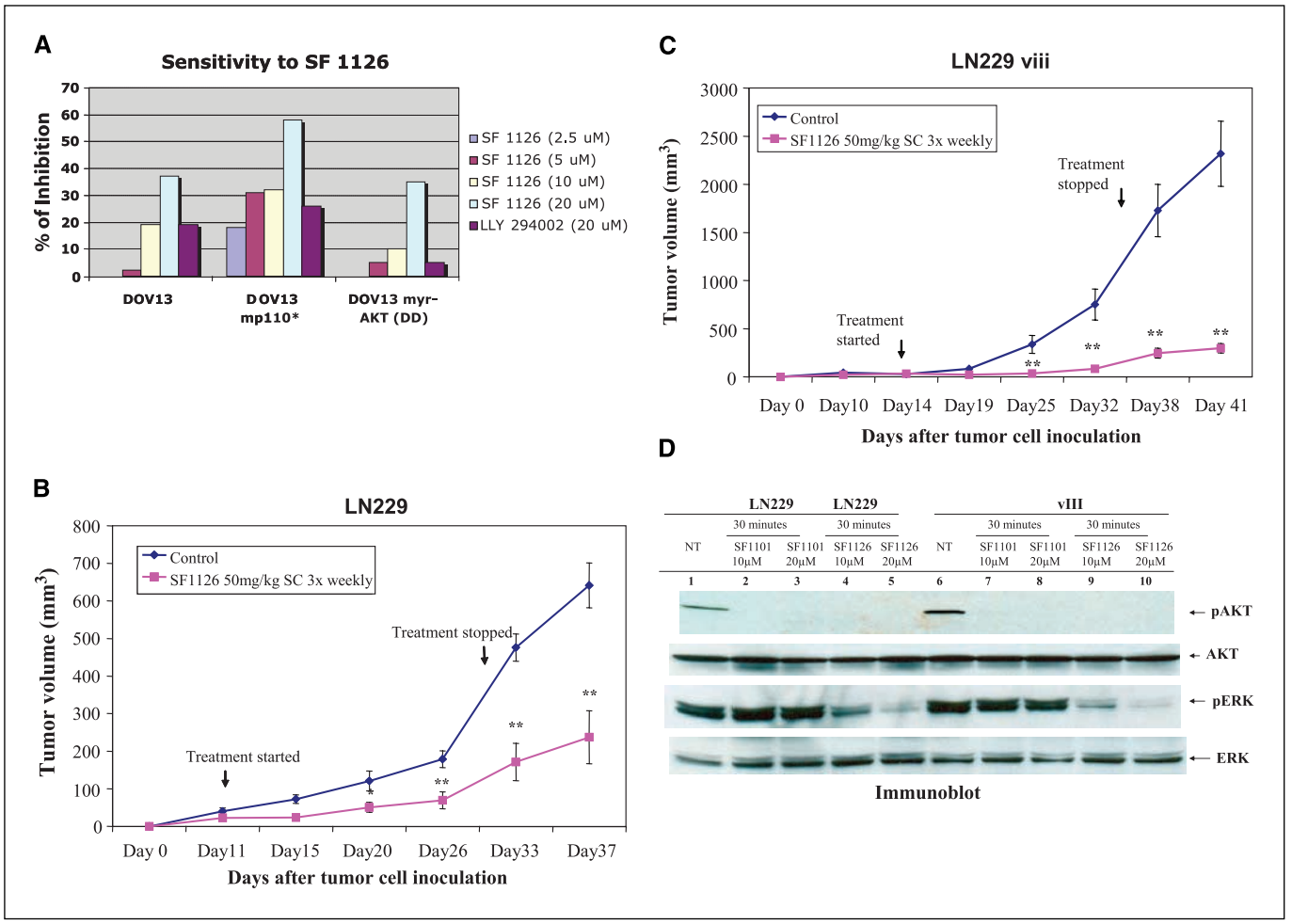

Figure 6. PI3K pathway activation predicts response to SF1126 therapy. We used isogenic tumor cell lines engineered to have greater activation of the PI3K or AKT signaling pathway to test the hypothesis that pathway activation/addiction makes tumors more sensitive to PI3K pathway inhibition by SF1126. *A,* DOV13, a human ovarian carcinoma cell line, was stably transduced with empty vector, p110CAAX, or caAKT. Sensitivity to apoptosis was examined *in vitro* for all three cell lines under conditions of SF1126 treatment. *B* and *C,* LN229 versus LN229 vIII as described above were implanted into nude mice. Biochemical analysis of PI3K-AKT signaling axis (9) confirms 3-fold to 4-fold augmentation in p-AKT in the LN229 vIII versus LN229 (*D*). Growth rate of tumors *in vivo* was significantly different. The relative response to SF1126 therapy was compared at 25 mg/kg/dose given MWF.

apoptotic pathway (30, 31), (*d*) BAD phosphorylation (32), (*e*) Myc via GSK3 and MIZ1 phosphorylation (33), (*f*) MDM2 (23–25), (*g*) 14-3-3 interaction with phosphorylated BAD, (*h*) RAF via PAK kinase (34), (*i*) TSC2-RHEB-mTOR-RS6 kinase (32), (*j*) Forkhead transcription factor (35), (*k*) ASK1 phosphorylation by AKT (36), and (*l*) p27 kip1 regulation (37). Thus, PI3K represents an important nodal point for the convergence of multiple cell surface receptors, which then leads to the downstream activation of multiple serine/threonine kinase cascades and the activation of multiple transcription factors.

It has been suggested that an important component of successful application of PI3K inhibitors to cancer therapeutics will be the capacity to measure the pharmacokinetic and pharmacodynamic effects of these agents *in vivo*. To this end, we have developed methods which allow us to quantitate SF1126/SF1101 concentrations in tumor tissue and plasma and to measure pharmacodynamic knockdown responses in tumor using biochemical and noninvasive PET imaging. The results show the capacity of SF1126 to affect a sustained knockdown of p-AKT and phosphorylated RS6 kinase for up to 12 h after the administration of this drug. To date, a limited number of preclinical studies with PTK inhibitors, e.g., Tarceva, have carefully examined the relationship between pharmacokinetic and pharmacodynamic knockdown of the target in tumor tissue (38). In some studies, a sustained knockdown of the target kinase activity is observed after the administration of kinase inhibitors despite a plasma and tumor half-life of this agent of 2 to 4 h (38). Hence, the relationship between pharmacokinetic and pharmacodynamic effects for a number of targeted therapeutic agents remains to be determined. The observed sustained knockdown of p-AKT and phosphorylated S6 kinase after a single dose of SF1126 supports the observed efficacy of SF1126 when given in an every other day schedule.

It is clear from the literature that multiple tumor types exhibit activation of the PI3K-AKT signaling axis either by PTEN loss or by incurring mutations in PIK3CA gene (39). We have now tested SF1126 against 11 different tumor cell lines representing seven different tumor lineages *in vivo* (Supplementary Fig. S5). Importantly, SF1126 displays significant single-agent antitumor activity against multiple glioblastoma cell lines, as well as prostate and breast cancer xenografts. We have determined activity of SF1126 against renal cell carcinoma, multiple myeloma, neuroblastoma, and rhabdomyosarcoma (Supplementary Fig. S5).[5] Importantly, SF1126, when combined with taxotere in a prostate cancer model (Supplementary Fig. S4), displays augmented antitumor activity *in vivo*. These results support the current focus, which is to use targeted therapeutic agents to modulate chemoradiosensitivity in cancer. In this way, SF1126, by virtue of its capacity to shut off a large number of downstream survival and proliferative signals in both tumor and stromal compartment, is an attractive signal modulator for other cytotoxic and genotoxic stressors.

It has been suggested by a number of investigators that tumors addicted to a specific biochemical pathway for growth, angiogenesis, and survival will display increased sensitivity to the inhibitors which attack this pathway (16, 17). We used isogenic tumor cell lines where the PTEN–PI3K-AKT axis is activated by different genetic manipulations to test *in vitro* or *in vivo* sensitivity to SF1126. The introduction of activated p110α catalytic subunit into DOV13 ovarian carcinoma cell line makes them more sensitive to SF1126 inhibitory activity *in vitro*. The transduction of activated myristoylated AKT, which is independent of PI3K for its activation into DOV13 cells, does not impart increased SF1126 sensitivity. Therefore, the upstream activation of PI3K or direct mutational activation of p110α results in cells which are more sensitive to pan PI3K inhibition. Finally, we introduced into LN229 glioma cells the EGFR vIII mutant receptor, which results in the constitutively activation of the PI3K pathway (9). The results suggest that the upstream activation of AKT via the mutated EGFR vIII as seen in GBM tumors results in more marked response to SF1126 *in vivo*.

Previous work from our laboratory established that the SF1101/LY294002 compound targets both the tumor and the stromal endothelial compartments (6). Because SF1126 is RGD-targeted to αvβ3 and α5β1 expressed on both endothelial and tumor cells, it was hypothesized that this agent might exert part of its antitumor activity based on its effects on the tumor microenvironment. Others have observed an effect of LY294002 on VEGF, HIF-1α, and p53 in the context of antiangiogenesis (6, 21, 24). Based on these prior results, we were interested in testing the SF1126 compound for antiangiogenic activity. Our results show that SF1126 has potent antiangiogenic activity in six different xenograft models tested thus far. To further study the action of SF1126 on angiogenesis, we examined its effect on a known positive regulator of tumor-induced angiogenesis, the HIF-1α transcription factor. We measured the hypoxic stabilization of HIF-1α protein in LN229 glioma cells by Western blot analysis. To further confirm this observation, we examined HIF-1α HRE-dependent transcription under hypoxic conditions. Similar results were observed with SF1126 treatment of glioma cells. From these data, we conclude that the PI3K pathway controls the hypoxic stabilization of HIF-1α in glioma cells. Moreover, both LY294002 and SF1126 block the hypoxic induction of HIF-1α transcription activity in these glioma cells. The mechanism by which PI3K or AKT regulate the hypoxic stability of HIF-1α is unclear (19). Preliminary evidence from our studies suggest that PI3K inhibitors may block the pathway by which HIF-1α is degraded under hypoxic conditions because MG132 blocks the effect of SF1126 on HIF-1α under hypoxic conditions (not shown).

In summary, we conclude that (*a*) SF1126 has potent antitumor activity against multiple human tumor types *in vivo*, (*b*) SF1126 has a favorable pharmacokinetic and pharmacodynamic effect on its target as indicated by inhibition of the downstream kinase, AKT *in vitro* and *in vivo*, (*c*) the RGD targeting moiety plays an important role in its *in vivo* and *in vitro* activity, and (*d*) SF1126 is well tolerated in mouse, rat, and canine models (data not shown). Moreover, we suggest that (*a*) FDG-PET should be evaluated in clinical trials to follow the therapeutic and pharmacodynamic response to PI3K inhibitor therapy *in vivo*, (*b*) tumor biopsies can be used to determine the degree of pathway inhibition potentially allowing dose modification or augmenting dose finding studies, (*c*) tumors with an activated PI3K-AKT signaling pathway are likely to be more sensitive to SF1126 potentially allowing for the enrichment of patients likely to respond in clinical trials, (*d*) SF1126 inhibits the hypoxic stabilization of HIF-1α signaling axis in tumor cells and is potently antiangiogenic *in vivo* suggesting an effect on the tumor microenvironment, and (*e*) SF1126 augments the antitumor activity of taxotere in a prostate cancer xenograft model. These combined results strongly suggest that SF1126 warrants testing as a single agent in human phase I/phase II clinical trials and subsequently in combinations with chemotherapy and radiation therapy. A clinical trial of SF1126 is now under way.

Acknowledgments

Received 2/19/2007; revised 8/3/2007; accepted 10/29/2007.

Grant support: CA94233 (D.L. Durden), P50CA83639 (G.B. Mills), and PO1CA099031 (G.B. Mills), Georgia Cancer Coalition, Aflac Cancer Center, and Semafore Pharmaceuticals.

The costs of publication of this article were defrayed in part by the payment of page charges. This article must therefore be hereby marked *advertisement* in accordance with 18 U.S.C. Section 1734 solely to indicate this fact.

We thank Qinghua Yu and Hassan Hall for excellent technical assistance, Dr. Erwin Van Meir for the provision of reagents, and all the dedicated people in Semafore and Durden laboratory for their commitment in bringing the first pan PI3K inhibitor into patient care.

References

1. Vlahos CJ, Matter WF, Hui KY, Brown RF. A specific inhibitor of phosphatidylinositol 3-kinase, 2-(4-morpholinyl)-8-phenyl-4H-1-benzopyran-4-one (LY294002). J Biol Chem 1994;269:5241–8.
2. Camps M, Ruckle T, Ji H, et al. Blockade of PI3Kγ suppresses joint inflammation and damage in mouse models of rheumatoid arthritis. Nat Med 2005;11:936–43.
3. Hayakawa M, Kaizawa H, Moritomo H, et al. Synthesis and biological evaluation of 4-morpholino-2-phenylquinazolines and related derivatives as novel PI3 kinase p110α inhibitors. Bioorg Med Chem 2006;14:6847–58.
4. Nutley BP, Raynaud FI, Hayes A, Goddard P, Jarman M, Workman P. Pharmacokinetics and metabolism of the phospatidylinositol 3-kinase inhibitor LY294002 in the mouse [abstract #2044]. Proc Am Assoc Cancer Res 92nd Annu Meet 2001;92:380.
5. Hu L, Zaloudek C, Mills GB, Gray J, Jaffe RB. *In vivo* and *in vitro* ovarian carcinoma growth inhibition by a phosphatidylinositol 3-kinase inhibitor (LY294002). Clin Cancer Res 2000;6:880–6.
6. Su JD, Mayo LD, Donner DB, Durden DL. PTEN and phosphatidylinositol 3′-kinase inhibitors up-regulate p53 and block tumor-induced angiogenesis: evidence for an effect on the tumor and endothelial compartment. Cancer Res 2003;63:3585–92.
7. Castellino RC and Durden DL. PTEN/PI-3 kinase signaling node: An intercept point for the control of angiogenesis. Nat Clin Pract Neurol. In press. 2007.
8. Katso R, Okkenhaug K, Ahmadi K, White S, Timms J, Waterfield MD. Cellular function of phosphoinositide 3-kinases: implications for development, homeostasis, and cancer. Annu Rev Cell Dev Biol 2001;17:615–75.
9. Li B, Yuan M, Kim IA, Chang CM, Bernhard EJ, Shu HK. Mutant epidermal growth factor receptor displays increased signaling through the phosphatidylinositol-3 kinase/AKT pathway and promotes radioresistance in cells of astrocytic origin. Oncogene 2004;23:4594–602.
10. Tan C, de Noronha RG, Roecker AJ, et al. Identification of a novel small-molecule inhibitor of the hypoxia-inducible factor 1 pathway. Cancer Res 2005;65:605–12.
11. Dey N, Howell BW, De PK, Durden DL. CSK negatively regulates nerve growth factor induced neural differentiation and augments AKT kinase activity. Exp Cell Res 2005;307:1–14.
12. Wen S, Stolarov J, Myers MP, et al. PTEN controls tumor-induced angiogenesis. Proc Natl Acad Sci U S A 2001;98:4622–7.
13. Sheehan KM, Calvert VS, Kay EW, et al. Use of reverse phase protein microarrays and reference standard development for molecular network analysis of metastatic ovarian carcinoma. Mol Cell Proteomics 2005;4:346–55.
14. Wong AJ, Ruppert JM, Bigner SH, et al. Structural alterations of the epidermal growth factor receptor gene in human gliomas. Proc Natl Acad Sci U S A 1992;89:2965–9.
15. Kanzaki M, Furukawa M, Raab W, Pessin JE. Phosphatidylinositol 4,5-bisphosphate regulates adipocyte actin dynamics and GLUT4 vesicle recycling. J Biol Chem 2004;279:30622–33.
16. Mills GB, Lu Y, Kohn EC. Linking molecular therapeutics to molecular diagnostics: inhibition of the FRAP/RAFT/TOR component of the PI3K pathway preferentially blocks PTEN mutant cells *in vitro* and *in vivo*. Proc Natl Acad Sci U S A 2001;98:10031–3.
17. Wendel HG, Malina A, Zhao Z, et al. Determinants of sensitivity and resistance to rapamycin-chemotherapy drug combinations *in vivo*. Cancer Res 2006;66:7639–46.
18. Evan GI. Can't kick that oncogene habit. Cancer Cell 2006;10:345–47.
19. Blancher C, Moore JW, Robertson N, Harris AL. Effects of ras and von Hippel-Lindau (VHL) gene mutations on hypoxia-inducible factor (HIF)-1α, HIF-2α, and vascular endothelial growth factor expression and their regulation by the phosphatidylinositol 3′-kinase/Akt signaling pathway. Cancer Res 2001;61:7349–55.
20. Zhong H, Chiles K, Feldser D, et al. Modulation of hypoxia-inducible factor 1α expression by the epidermal growth factor/phosphatidylinositol 3-kinase/PTEN/AKT/FRAP pathway in human prostate cancer cells: implications for tumor angiogenesis and therapeutics [in process citation]. Cancer Res 2000;60:1541–5.
21. Huang J, Kontos CD. PTEN modulates vascular endothelial growth factor-mediated signaling and angiogenic effects. J Biol Chem 2002;277:10760–6.
22. Hu L, Hofmann J, Lu Y, Mills GB, Jaffe RB. Inhibition of phosphatidylinositol 3′-kinase increases efficacy of paclitaxel in *in vitro* and *in vivo* ovarian cancer models. Cancer Res 2002;62:1087–92.
23. Mayo L, Donner D. The PTEN, Mdm2, p53 tumor suppressor-oncoprotein network. Trends Biochem Sci 2002;27:462–5.
24. Mayo LD, Dixon JE, Durden DL, Tonks NK, Donner DB. PTEN protects p53 from Mdm2 and sensitizes cancer cells to chemotherapy. J Biol Chem 2002;277:5484–9.
25. Mayo LD, Donner DB. A phosphatidylinositol 3-kinase/Akt pathway promotes translocation of Mdm2 from the cytoplasm to the nucleus. Proc Natl Acad Sci U S A 2001;98:11598–603.
26. Gottschalk AR, Doan A, Nakamura JL, Haas-Kogan DA, Stokoe D. Inhibition of phosphatidylinositol-3-kinase causes cell death through a protein kinase B (PKB)-dependent mechanism and growth arrest through a PKB-independent mechanism. Int J Radiat Oncol Biol Phys 2005;61:1183–8.
27. Gottschalk AR, Doan A, Nakamura JL, Stokoe D, Haas-Kogan DA. Inhibition of phosphatidylinositol-3-kinase causes increased sensitivity to radiation through a PKB-dependent mechanism. Int J Radiat Oncol Biol Phys 2005;63:1221–7.
28. Nakamura JL, Karlsson A, Arvold ND, et al. PKB/Akt mediates radiosensitization by the signaling inhibitor LY294002 in human malignant gliomas. J Neurooncol 2005;71:215–22.
29. Ozes ON, Mayo LD, Gustin JA, Pfeffer SR, Pfeffer LM, Donner DB. NF-κB activation by tumour necrosis factor requires the Akt serine-threonine kinase [see comments]. Nature 1999;401:82–5.
30. Goswami A, Burikhanov R, de Thonel A, et al. Binding and phosphorylation of par-4 by akt is essential for cancer cell survival. Mol Cell 2005;20:33–44.
31. Goswami A, Ranganathan P, Rangnekar VM. The phosphoinositide 3-kinase/Akt1/Par-4 axis: a cancer-selective therapeutic target. Cancer Res 2006;66:2889–92.
32. Inoki K, Li Y, Zhu T, Wu J, Guan KL. TSC2 is phosphorylated and inhibited by Akt and suppresses mTOR signalling. Nat Cell Biol 2002;4:648–57.
33. Wanzel M, Kleine-Kohlbrecher D, Herold S, et al. Akt and 14-3-3eta regulate Miz1 to control cell-cycle arrest after DNA damage. Nat Cell Biol 2005;7:30–41.
34. King AJ, Sun H, Diaz B, et al. The protein kinase Pak3 positively regulates Raf-1 activity through phosphorylation of serine 338. Nature 1998;396:180–3.
35. Medema RH, Kops GJ, Bos JL, Burgering BM. AFX-like Forkhead transcription factors mediate cell-cycle regulation by Ras and PKB through p27kip1. Nature 2000;404:782–7.
36. Zhang L, Chen J, Fu H. Suppression of apoptosis signal-regulating kinase 1-induced cell death by 14-3-3 proteins. Proc Natl Acad Sci U S A 1999;96:8511–5.
37. Fujita N, Sato S, Katayama K, Tsuruo T. Akt-dependent phosphorylation of p27Kip1 promotes binding to 14-3-3 and cytoplasmic localization. J Biol Chem 2002;277:28706–13.
38. Thomas SM, Grandis JR. Pharmacokinetic and pharmacodynamic properties of EGFR inhibitors under clinical investigation. Cancer Treat Rev 2004;30:255–68.
39. Cantley LC, Neel BG. New insights into tumor suppression: PTEN suppresses tumor formation by restraining the phosphoinositide 3-kinase/AKT pathway. Proc Natl Acad Sci U S A 1999;96:4240–5.

Correction: Pan PI3K Inhibitor Prodrug for Cancer Therapy

The article on pan PI3K inhibitor prodrug for cancer therapy in the January 1, 2008 issue of *Cancer Research* (1) should have included the following conflict of interest statement: D.L. Durden would like to disclose a financial interest in Semafore Pharmaceuticals. The terms of the arrangement have been reviewed and approved by Emory University in accordance with the conflict of interest policies.

1. Garlich JR, De P, Dey N, Su JD, Peng X, Miller A, Murali R, Lu Y, Mills GB, Kundra V, Shu H-K, Peng Q, Durden DL. A vascular targeted pan phosphoinositide 3-kinase inhibitor prodrug, SF1126, with antitumor and antiangiogenic activity. Cancer Res 2008;68:206–15.

doi:10.1158/0008-5472.CAN-68-14-COR1

A Vascular Targeted Pan Phosphoinositide 3-Kinase Inhibitor Prodrug, SF1126, with Antitumor and Antiangiogenic Activity

Joseph R. Garlich, Pradip De, Nandini Dey, et al.

Cancer Res 2008;68:206-215.